Transactions of the Korean Nuclear Society Autumn Meeting
Gyeongju, Korea, October 29-30, 2015

Finite Element Analysis for Bending Process of U-Bending Specimens

Won Dong Park[a], Chi Bum Bahn [a*]
[a]*Pusan National University, 2Busandaehak-ro 63beon-gil, Geumjeong-gu, Busan 609-735, Republic of Korea*
**Corresponding author: bahn@pusan.ac.kr*

1. Introduction

To perform the Primary Water Stress Corrosion Cracking (PWSCC) initiation testing, U-bend specimens have been used [1]. It is known that the applied stress/strain including residual stress/strain is directly related to PWSCC initiation time [2]. Therefore, it is necessary to know the exact stress/strain state of the U-bend specimens for predicting PWSCC initiation time.

It is known that the crack initiation occurs approximately after 10^3 hours when true stress range is from 600 to 700 [3]. To apply this result to calculating true stress/strain state, it is necessary to restrict PWSCC initiation time within 10^3 hours.

ASTM G30 [1] suggests that the applied strain can be calculated by dividing thickness by a bend radius. It should be noted, however, that the formula is reliable under an assumption that the ratio of thickness to bend radius is less than 0.2. Typically, to increase the applied stress/strain, the ratio of thickness to bend radius becomes larger than 0.2. This suggests that the estimated strain values by ASTM G30 are not reliable to predict the actual residual strain state of the highly-deformed U-bend specimen. For this reason, finite element analysis (FEA) for the bending process of U-bend specimens was conducted by using a commercial finite element analysis software ABAQUS. ver.6.14-2;2014 [4].

From the results of FEA, PWSCC initiation time and U-bend specimen size can be determined exactly.

2. Finite element analysis procedure

In this section, the FEA procedure for U-bend specimens is described. As shown Table I, cases were divided according to bend radius, distance of two rollers and thickness of specimen. The estimated strain from ASTM G30 is also shown for each case.

Table Ⅰ: Bend radius and thickness data used in each analysis case

	Bend radius (R,mm)	Thickness (T,mm)	Distance of two rollers (D,mm)	Estimated strain(ε) from ASTM G30
Case 1	8.3	2	30.6	0.12
Case 2	7.81	3	31.63	0.19
Case 3	8.3	3	32.6	0.18

Table Ⅱ: Properties of Alloy 182

Alloy 182	Properties	Source of data
Young's modulus(E)	184 GPa	True stress vs. True strain curve[Fig. 1]
Yield stress	381 MPa	
Poison's rate(v)	0.32	[5]
Density	8.47E-006 kg/mm^3	[6]

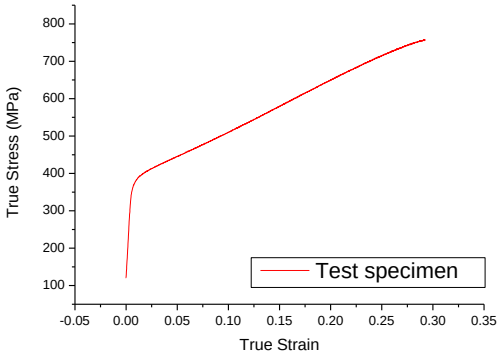

Fig. 1 True stress vs. true strain curve of Alloy 182.

Table II shows mechanical and physical properties of Alloy 182 used in FEA. Figure 1 shows the true stress vs. true strain curve of Alloy 182, which was acquired from a tensile test.

C3D8R element was used for the element type. C3D8R means 8-node linear brick reduced integral elements [4] .In addition, material was set to have isotropic elastic and isotropic plastic hardening characteristics.

In order to represent the U-bending process using a bending jig, steps were divided into 4 stages (See Fig. 2). First, the boundary conditions fixing position of parts was set in step 1. Second, the bending process of controlling roller's displacement located in the center of roller was done in step 2. Third, the fixing the U-bend legs process was performed in step 3. Finally, specimen was separated from the jig which is stationary in step 4 (See Table III).

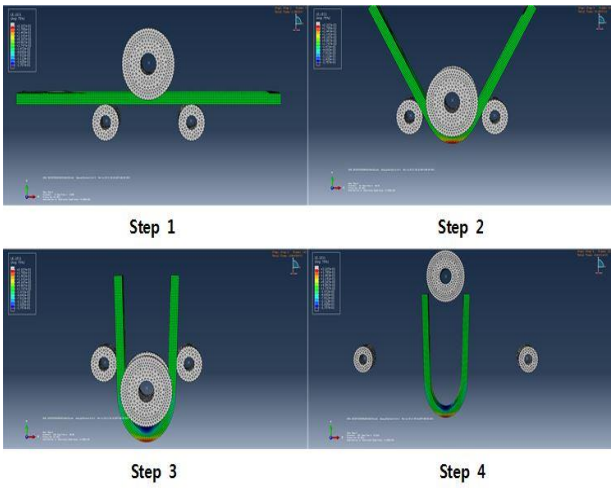

Fig. 2 U-bending specimen was bent according to each step.

Table Ⅲ: Required time and process in accordance with steps

	Required time (sec)	Process
Step 1	0 ~ 1	Fixing the position of parts
Step 2	1 ~ 101	Bending the specimen
Step 3	101 ~ 201	Fixing the U-bend legs
Step 4	201 ~ 202	Separate the specimen from the jig in the two sides are stationary

3. Finite element analysis results

3.1 Strain analysis

Figure 3 shows strain distribution after bending specimen. In all cases, specimens transformed to saddle shape and maximum strain was occurred in point ‘a’, ‘b’.

Figure 4 shows that maximum strains were occurred at 45 s, 48 s, and 63 s (0.15, 0.21, and 0.21 respectively) and sustained almost constant value after maximum strain time. But strains were slightly decreased after maximum strain time. This strain reduction seems to cause significant stress change.

Figures. 5 and 6 show strain distribution in the line 1 (from ‘a’ to ‘b’) and line 2 (from ‘c’ to ‘d’). In the lights of the results that the strain of case 2 (relatively thick) are higher than case 1 (relatively thin), it is thought that the thickness has a significant effect on maximum strain value.

In the table IV, estimated strains are compared with FEA strains. Average strains were almost similar. But estimated strains by ASTM G30 [1] were underestimated comparing to the maximum strains calculated by FEA. On the other hand, minimum strains were over-estimated.

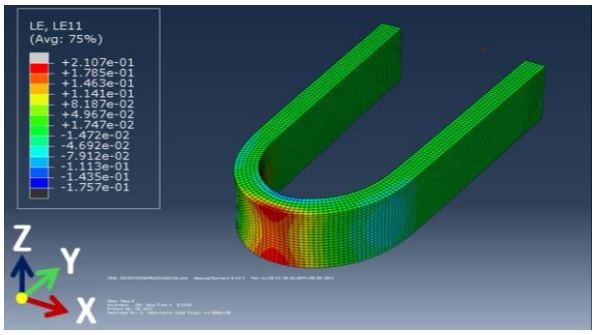

Fig. 3 X-axis direction strain distribution (LE11, case 3).

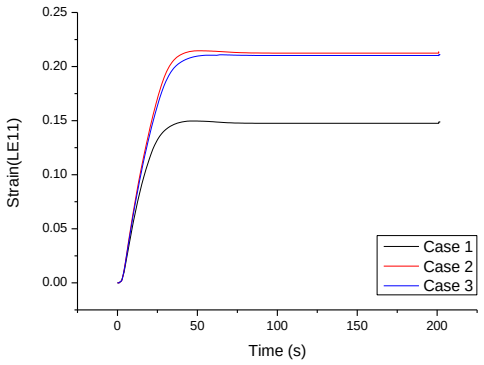

Fig. 4 X-axis direction strain history of each case at point ‘a’ (S11).

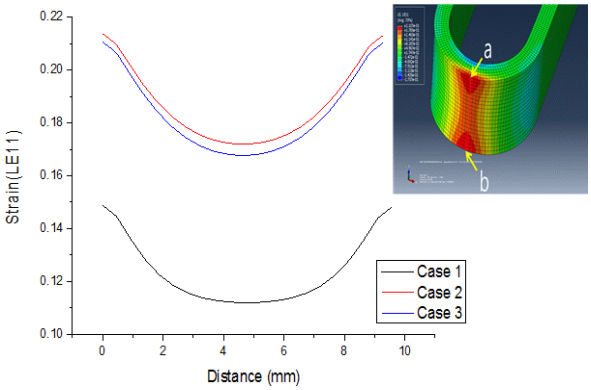

Fig. 5 Strain distribution of each case along the line from ‘a’ to ‘b’.

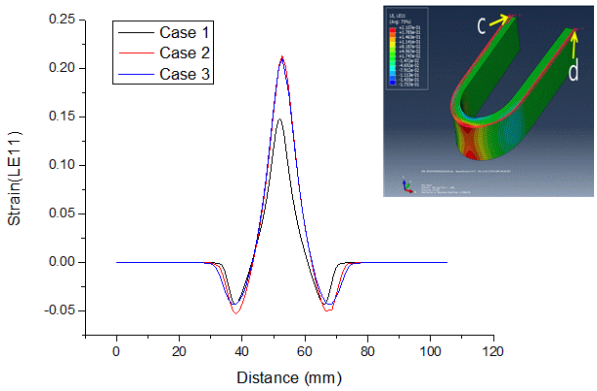

Fig. 6 Strain distribution of each case along the line from ‘c’ to ‘d’.

Table Ⅳ: FEA vs. Estimated Strains

	Estimated strain (ε_E)	FEA strain (ε_{FEA})		
		Max	Avg	Min
Case 1	0.12	0.15	0.12	0.11
Case 2	0.19	0.21	0.19	0.17
Case 3	0.18	0.21	0.18	0.17

3.2 Stress analysis

When the specimen was bent, stresses were concentrated in the point ‘a’, ‘b’ (See Figs. 7, 8 and 9). And the maximum tensile stress (x-axis direction) was occurred near the point ‘a’, ‘b’ (See Figs. 7 and 8). At the same time, the maximum compression stress (z-axis direction) was occurred near the center of line 2 (See Fig. 9). This means that crack initiation can arise near the point ‘a’, ‘b’. So it is anticipated that the most of cracks’ direction will be determined by x-axis stress.

Figures. 10 and 11 show that the stress was dramatically changed and recovered at point ‘a’. This means that slight reduction of strain caused immense change of stress (See Fig. 4). It seems that relative position between the specimen and the roller was changed and constraint condition was also changed as time goes on.

Figures. 12 and 13 show stress distribution of each case depending on distance through line 1, line 2 respectively. Stress in case 3 was higher than the others on the line 1 and line 2. These results correspond to intended residual stress.

On the other hand the final residual stress was recovered to almost maximum stress (670 MPa) in the case 3 whereas case 1 and 2 was not recovered (See Figs. 10 and 11). It seems to be occurred elastic relaxation due to spring back in step 2. This phenomenon can causes inaccuracy in intended final residual stress. Therefore, it is necessary that intended final residual stress be made by controlling the displacement of the U-bend legs and giving the stress to specimen again. By giving additional stress to specimen, specimens of Case 1 and Case 2 can recover their residual stress up to maximum stress.

As considering the distribution behavior of these residual stresses, it is determined that the case 3 which has a small stress spring back while making the specimen is suitable.

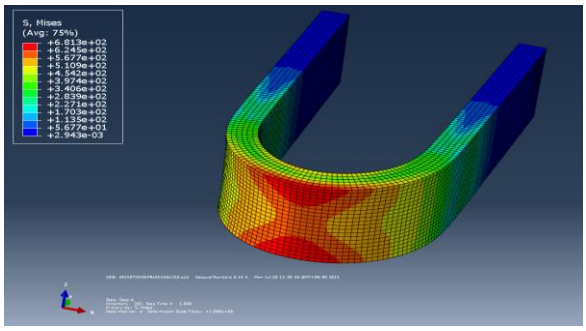

Fig. 7 Equivalent stress distribution (Von Mises, case 3).

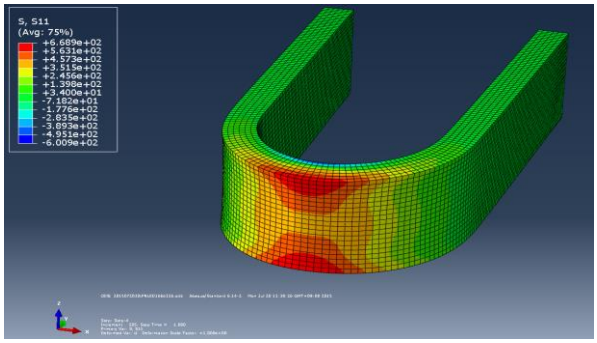

Fig. 8 X-axis direction stress distribution (S11, case 3).

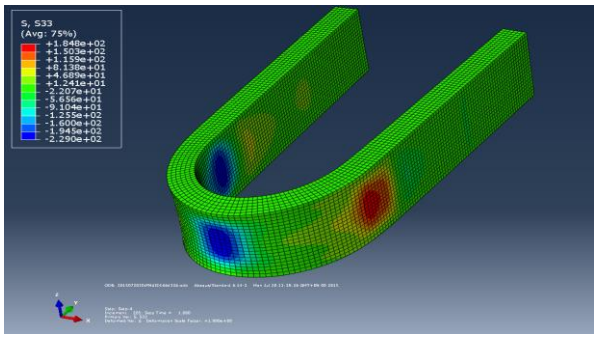

Fig. 9 Z-axis direction stress distribution (S33, case 3).

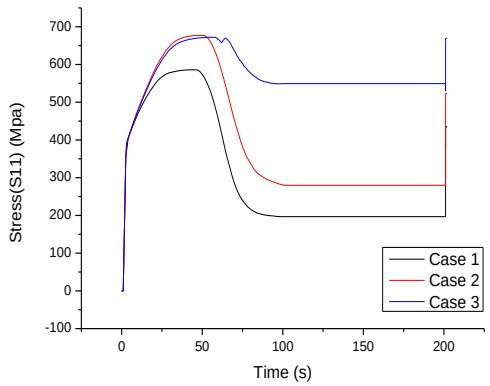

Fig. 10 X-axis direction stress history of each case at point ‘a’ (0~200s).

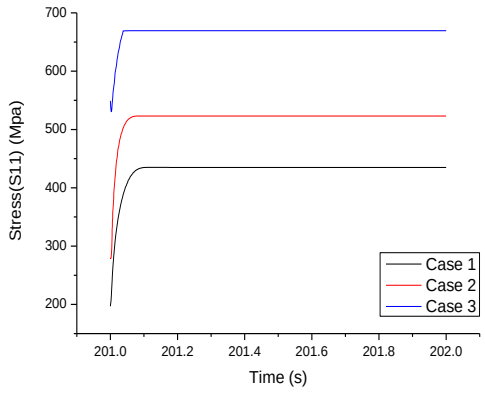

Fig. 11 X-axis direction stress history of each case at point 'a' (201~202s)

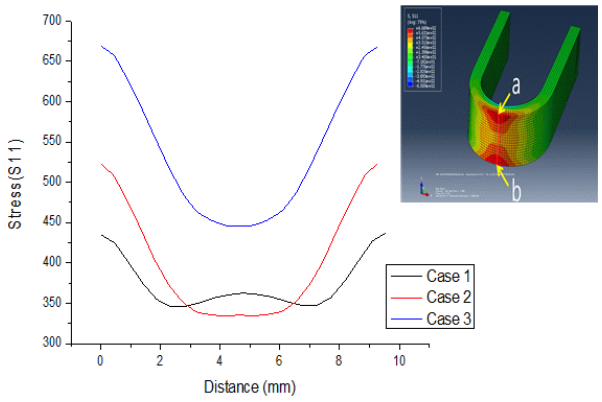

Fig. 12 Stress distribution of each case along the line from 'a' to 'b'.

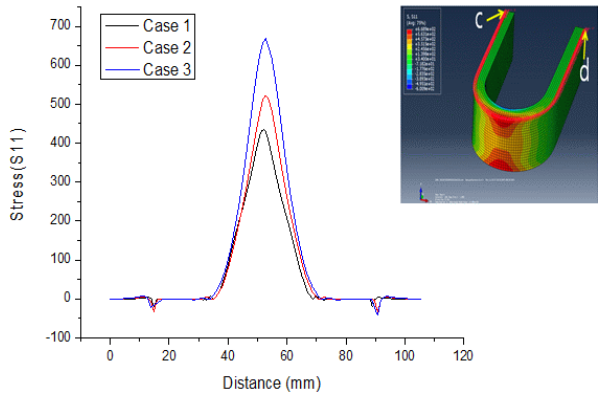

Fig. 13 Stress distribution of each case along the line from 'c' to 'd'.

3. Conclusions

To determine the exact stress/strain state of U-bending specimens for PWSCC test, FEA U-bending process simulation was carried out. By bending specimens like a U shape, sufficiently large stress and strain can be applied to specimens. Although averaged strains from FEA were similar to estimated strains from ASTM G30 [1], maximum and minimum strains from FEA were significantly different from .

Since local stress and strain have a significant effect on the initiation of PWSCC, it was inappropriate to apply results of ASTM G30 to the PWSCC test directly.

According to results of finite element analysis (FEA), elastic relaxation can cause inaccuracy in intended final residual stress. To modify this inaccuracy, additional process reducing the spring back is required. However this additional process also may cause uncertainty of stress/strain state. Therefore, the U-bending specimen size which is not creating uncertainty should be optimized and selected.

With the bending radius of 8.3 mm, the thickness of 3 mm and the roller distance of 32.6 mm, calculated maximum stress and strain were 670 MPa and 0.21, respectively. Under these stress and strain conditions, it is expected to have crack initiation time in PWSCC test within a reasonable time frame (~1,000 hours).

Acknowledgements

This work was supported by the Nuclear Safety Research Program through the Korea Radiation Safety Foundation(KORSAFs) and the Nuclear Safety and Security Commission(NSSC), Republic of Korea (Grant No, 1403006)

REFERENCES

[1] American Society for Testing and Materials(ASTM) International, ASTM G 30-97(Reapproved 2009) Standard Practice for Making and Using U-Bend Stress-Corrosion Test specimens, 2009.

[2] P. Scott, et al. "Comparison of Laboratory and Field Experience of PWSCC in Alloy 182 Weld Metal," Proc. 13th Int. Conf. on Environmental Degradation of Materials in Nuclear Power Systems, Whistler, British Columbia, August 19-23, 2007.

[3] "PWSCC/LPSCC in PWRs (+ Steam Generator Corrosion)," USNRC, Adams No. ML11266A011

[4] Simulia ABAQUS User's Manuals. Ver.6.14-2; 2014.

[5] J.-D. Hong, et al., "PFM Application for the PWSCC Integrity of Ni-Base Alloy Welds-Development and Application of PINEP-PWSCC," Nucl. Eng. Tech. 44 (2012) 961-970.

[6] J. S. Kim, J. H. Seo, "A study on welding residual stress analysis of a small bore nozzle with dissimilar metal welds," International Journal of Pressure Vessel and Piping, 90-91(2012) 69-76.